

LATE CRETACEOUS – EARLY PALEOGENE TECTONIC EVOLUTION OF THE CENTRAL PAMIR

INFERRED FROM GEOCHEMICAL FEATURES OF BARTANG VOLCANICS

Jovid Aminov^{1,2}, Guillaume Dupont-Nivet^{3,4}, Ding Lin², Stephane Guillot⁵, Johannes Glodny⁶, Carole Cordier⁵, Pierrick Roperch⁴, Yunus Mamadjanov^{1,7}, Mamurjon Mirvaisov⁸

¹Institute of Geology, Earthquake Engineering and Seismology, Academy of Sciences of the Republic of Tajikistan, Dushanbe, Tajikistan,

²Key Laboratory of Continental Collision and Plateau Uplift, Institute of Tibetan Plateau Research, Center for Excellence in Tibetan Plateau Earth Sciences, Chinese Academy of Sciences, Beijing 100101, China,

³ Institut für Geowissenschaften, Universität Potsdam, Potsdam, Germany,

⁴Géosciences Rennes, Univ. Rennes, CNRS, Rennes, France,

⁵Univ. Grenoble Alpes, Univ. Savoie Mont-Blanc, CNRS, IRD, IFSTTAR, Grenoble, France,

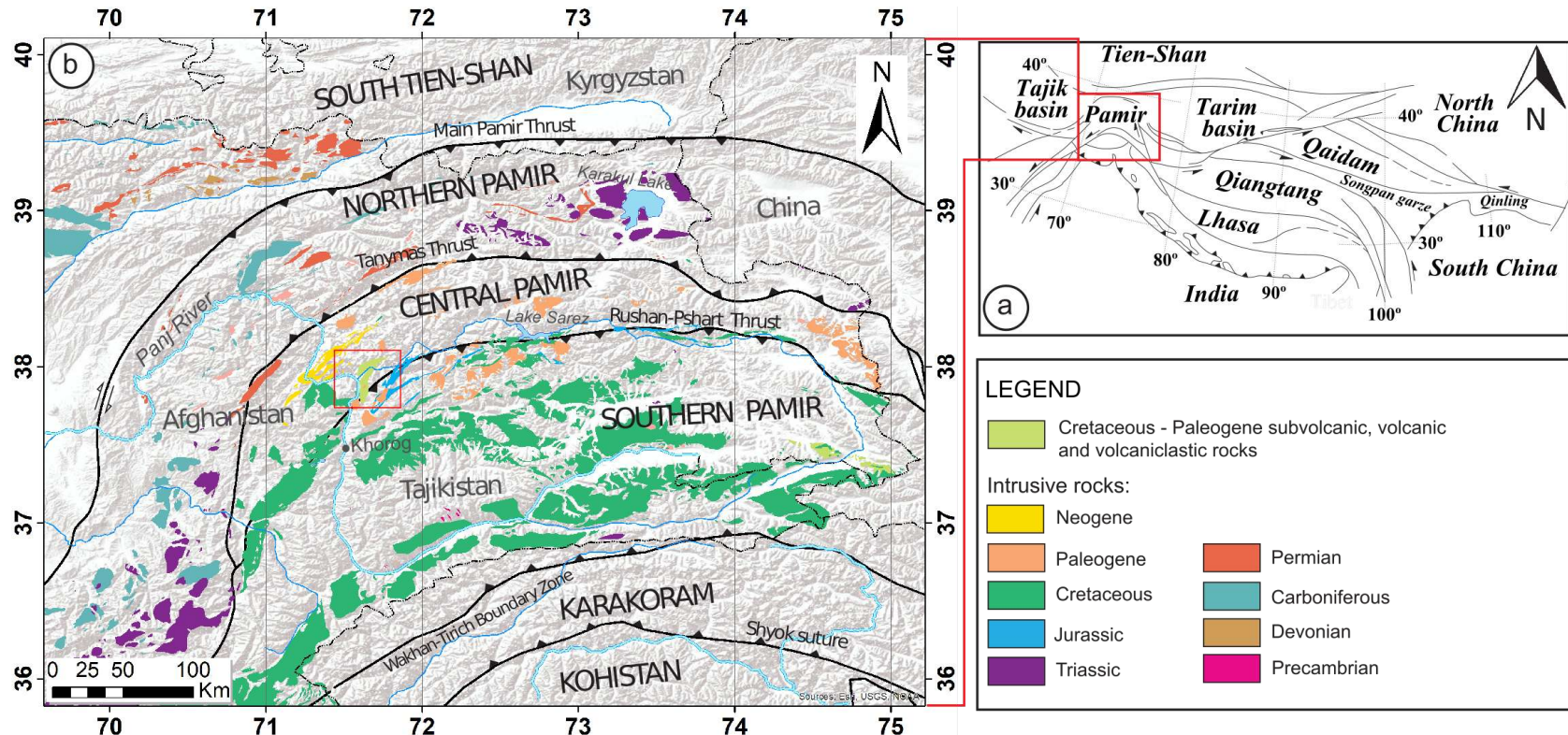
⁶Deutsches GeoForschungsZentrum GFZ, Telegrafenberg, D-14473 Potsdam, Germany,

⁷Research Center for Ecology and Environment of Central Asia, Dushanbe, Tajikistan,

⁸Academy of Sciences of the Republic of Tajikistan, Dushanbe, Tajikistan

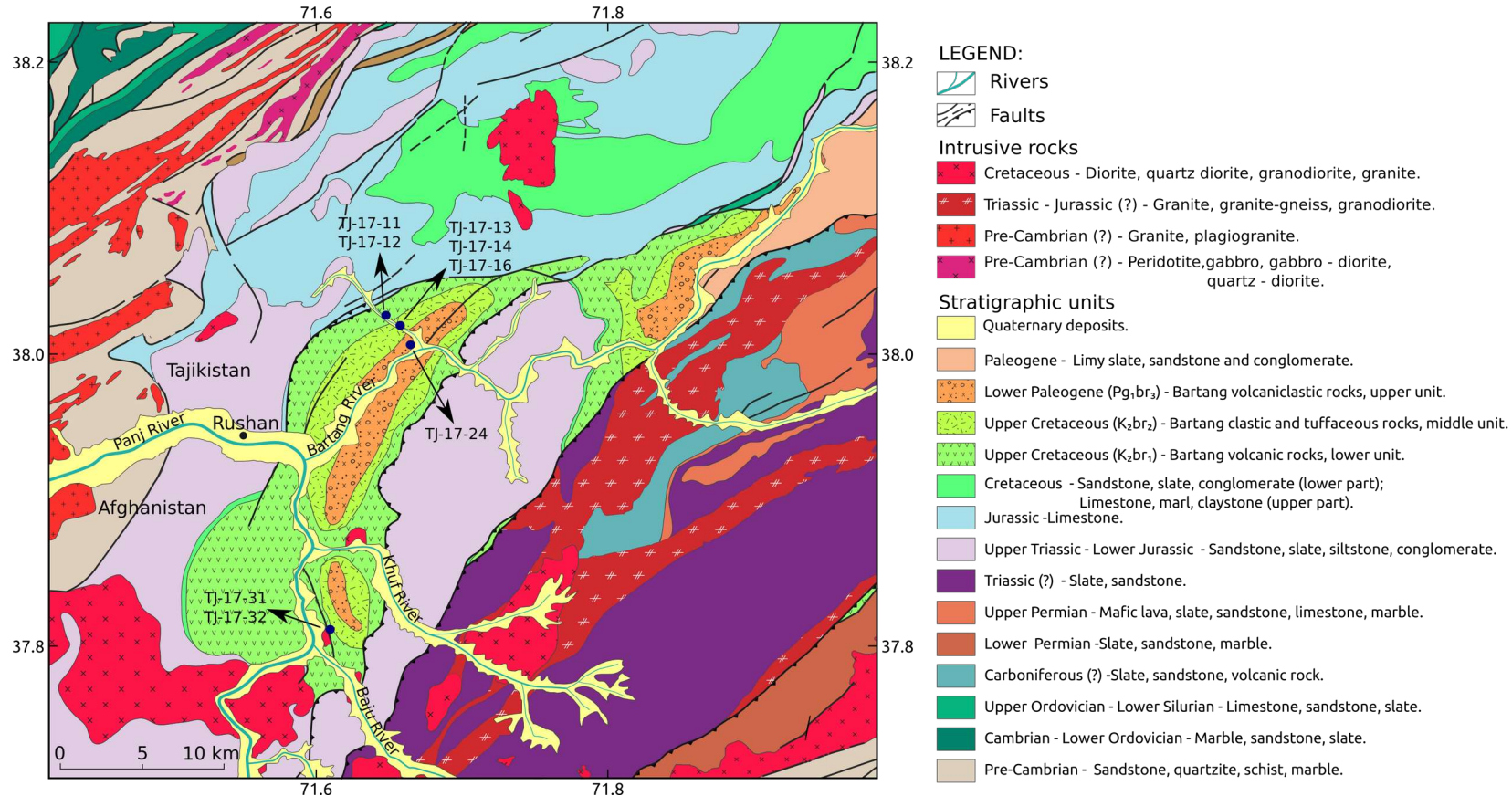
Tectonic map of the Pamir, showing distribution of igneous rocks.

Bartang volcanic and volcanoclastic rocks crop out in the western part of the Central Pamir (red square). During the Cretaceous the Southern Pamir was a site of widespread arc-related magmatism. However, the Central Pamir remained magmatically inactive until the late Cretaceous, when the Bartang volcanics and intruding plutons formed.

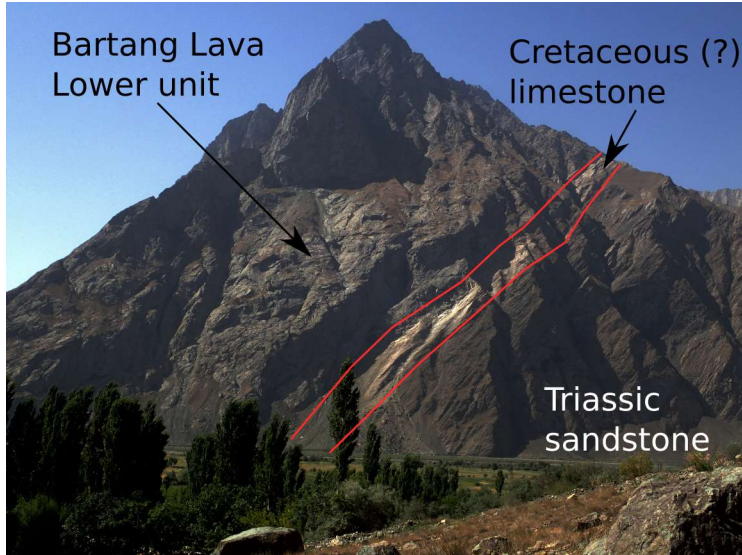


Geological map of the Bartang sequence.

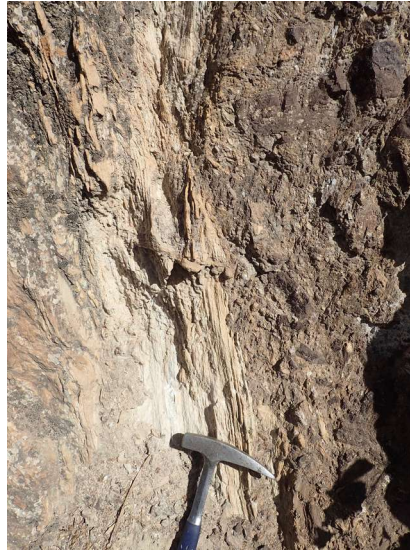
The Bartang sequence is divided into three units, which have distinct lithology. The lower unit, which comprises mafic and intermediate lavas and tuff, is intruded by late Cretaceous plutons of diorite and granite. The location of samples, which were analyzed for geochemical composition, radiogenic isotope ratios (Sr-Nd) and Zircon U/Pb ages, is shown by blue circles.



Outcrop photos.



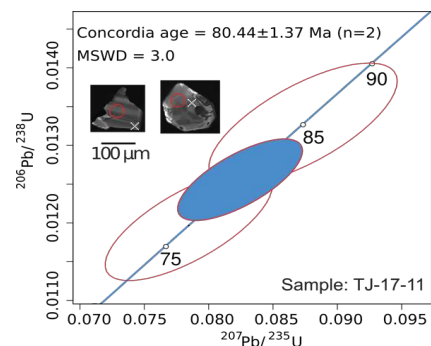
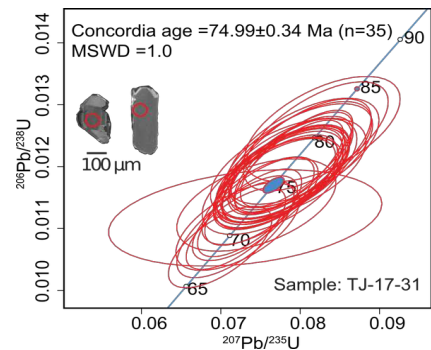
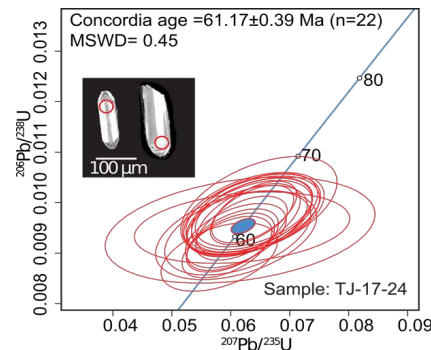
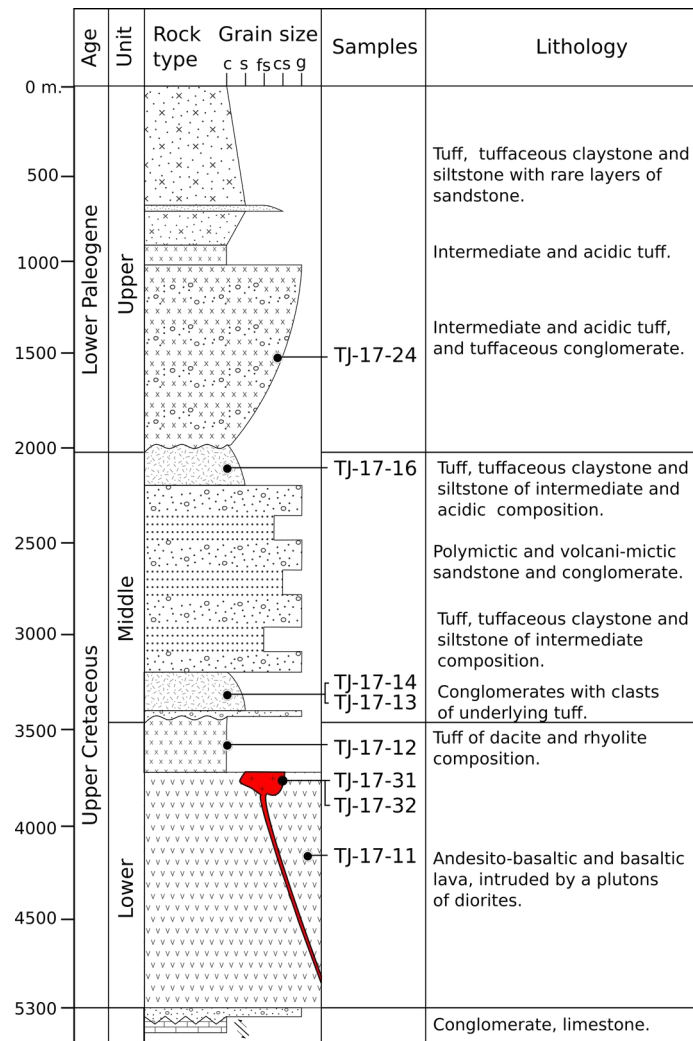
Volcanic rocks of Bartang sequence unconformably lie on a bed of limestone of Cretaceous (?) age. Lava forms massive layers.



The basal layer of volcanic rocks consists of conglomerate and breccia that contains limestone and sandstone clasts of underlying deposits



Tuffaceous rocks form thin layers intercalating with lava.



Stratigraphy and age.

The Bartang sequence comprises three units, which contain several distinct layers each. The units are separated from each other by erosion surfaces and stratigraphic unconformities.

We dated 4 samples from the Bartang sequence. The oldest age – 80 Ma, although with only two zircon grains was obtained from sample TJ-17-11, a mafic lava sampled from the lower unit. A diorite pluton that intrudes the lower unit yielded ages of 75 Ma from two samples – TJ-17-31, TJ-17-32.

A crystal-lithic tuff from the upper unit - TJ-17-24 yielded a concordia age of 61 Ma.

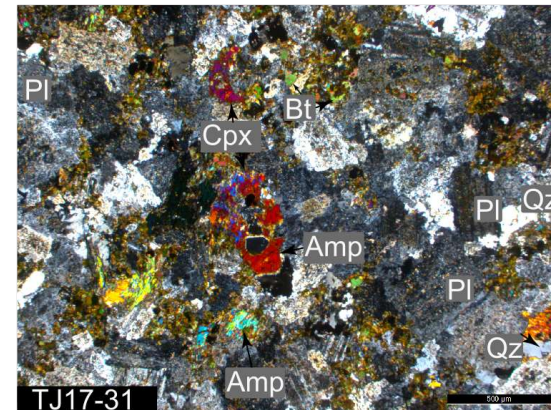
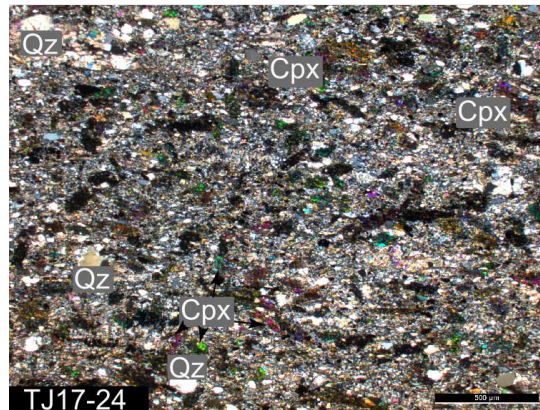
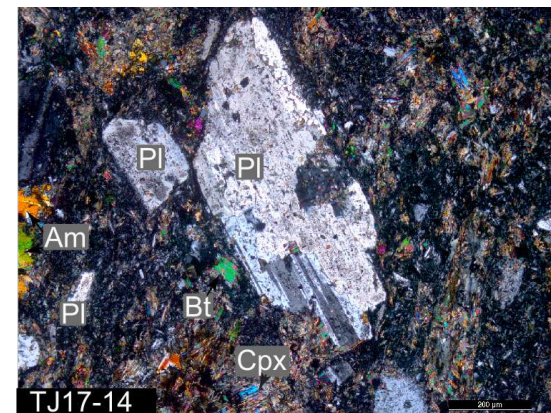
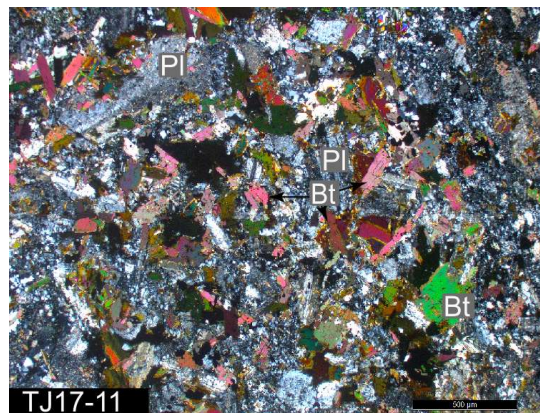
Petrography.

A mafic lava from the lower unit of the Bartang sequence - TJ-17-11 has a porphyritic texture, containing large, eu- to subhedral plagioclase phenocrysts and smaller biotite crystals set in a fine-grained groundmass of probably the same minerals.

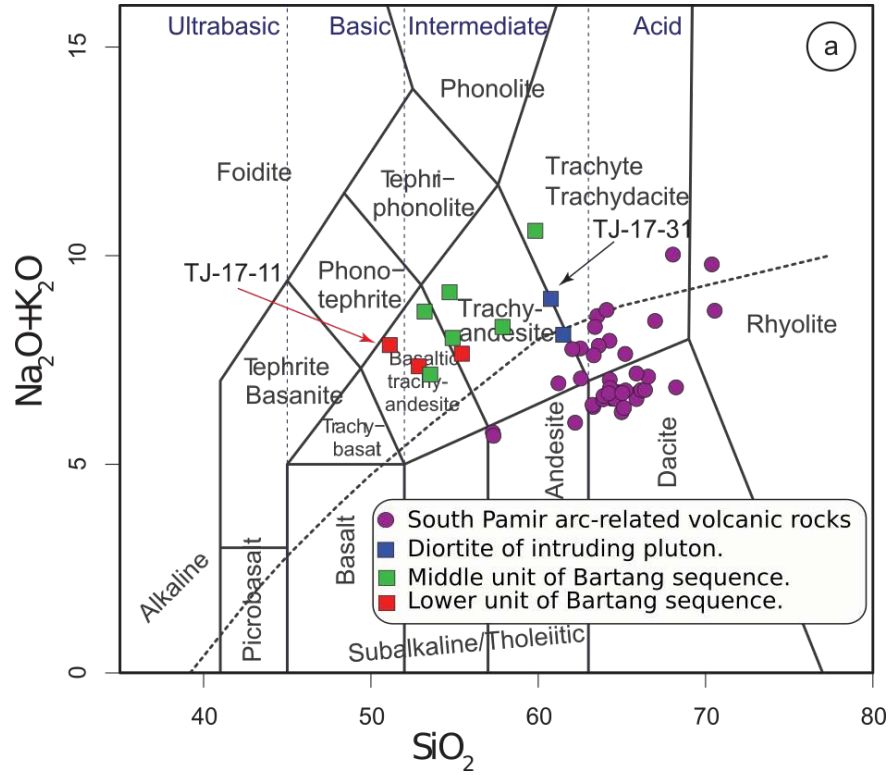
A crystalline tuff sampled from the middle unit - TJ-17-14 contains large crystals of subhedral plagioclase and smaller amphibole crystals embedded in a cryptocrystalline groundmass. Fine-grained biotite crystals seem to be secondary and develop over the clinopyroxene and plagioclase grains.

TJ-17-24 is a crystal-lithic tuff sampled from the upper unit and contains clinopyroxene, quartz and to a smaller extent mica, plagioclase and lithic fragments of sandstone and limestone.

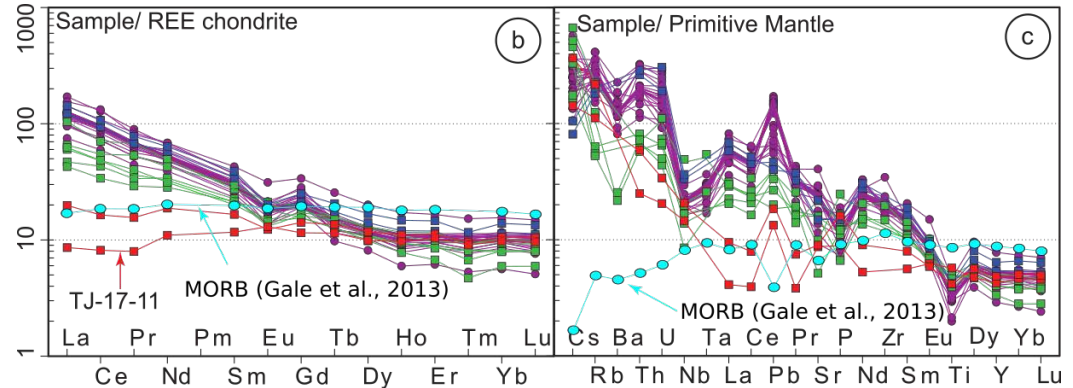
Diorite from the pluton that intrudes the lower unit - TJ-17-31 contains coarse eu- to subhedral feldspar crystals in association with subhedral amphibole, clinopyroxene and quartz grains. In this sample, sericite occasionally replaced feldspar.

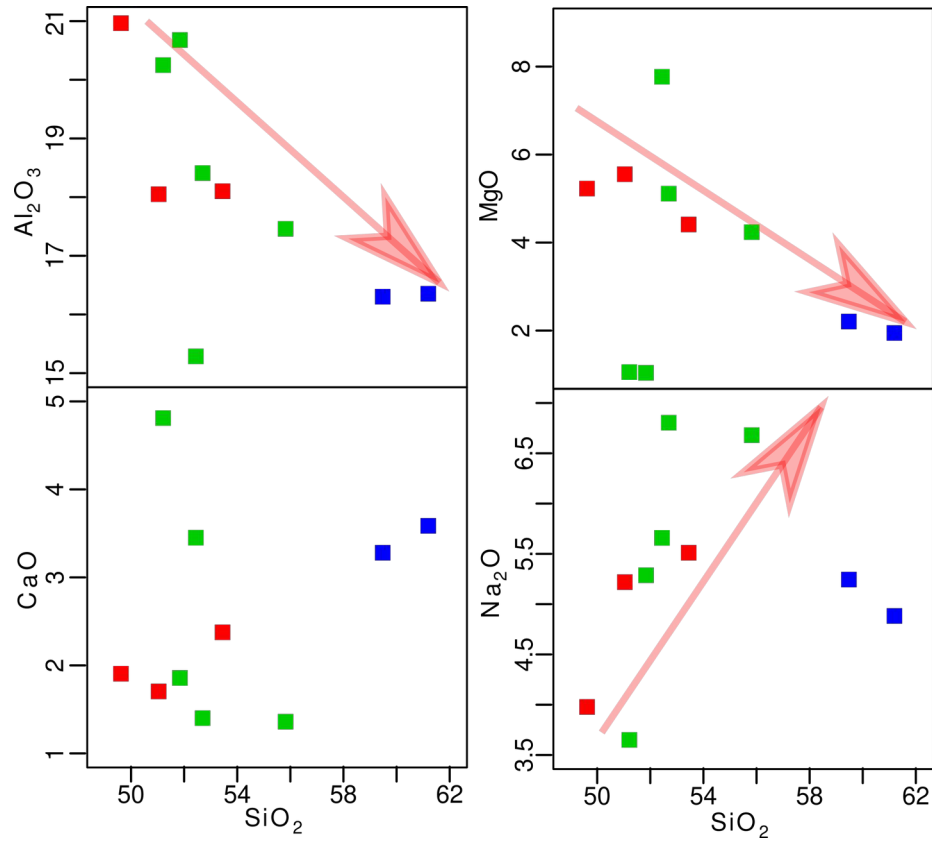


Geochemistry.



(a) TAS diagram classifying the volcanic samples as basaltic trachyandesite, trachyandesite and trachydacite, with the samples TJ-17-11 plotting in the mafic field and other samples in the intermediate. REE (b) and trace elements (c) compositions normalized relative to chondrite (Boynton, 1984) and primitive mantle (McDonough & Sun, 1995) respectively. REE patterns of the lavas of lower unit are similar to MORB with Light Rare Earth Elements depleted. However, trace elements normalized to primitive mantle show enrichment of the rocks in elements highly mobile in fluids (Rb, Ba, Pb) and in highly incompatible elements (Nb, Th, U). The samples have positive Pb anomaly suggesting derivation from metasomatized mantle source. The south Pamir mid-Cretaceous volcanic rocks are shown for comparison.



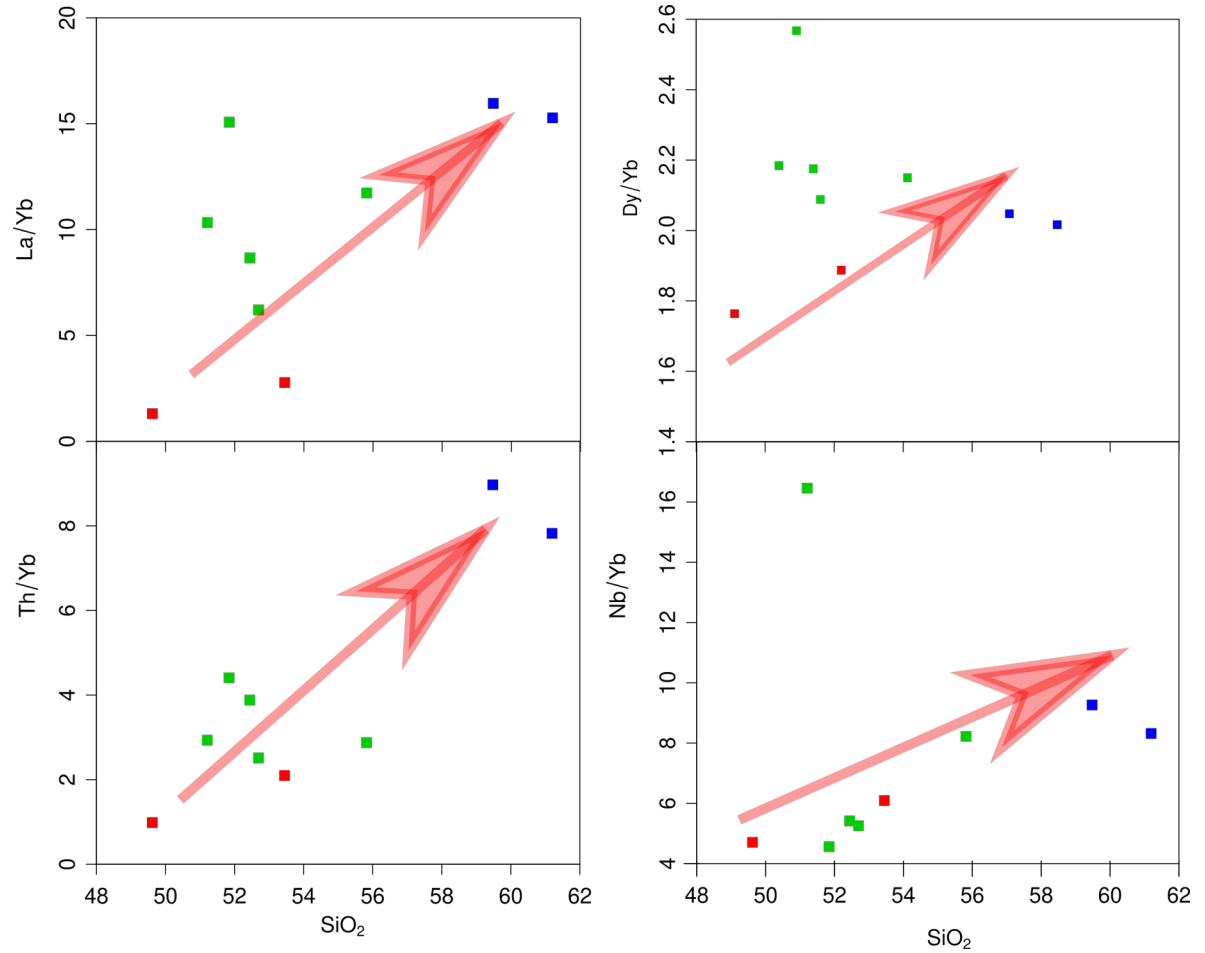


Geochemistry.

Major elements correlation diagrams of Bartang volcanic and plutonic rocks. Positive correlation between Na_2O and SiO_2 is clear, although the plutons (blue) plot out of the trend. Negative correlation between MgO and SiO_2 , and between SiO_2 and Al_2O_3 indicate fractional crystallization of mafic minerals and fractionation of plagioclase and (or garnet) respectively. Correlation between SiO_2 and CaO is not very clear.

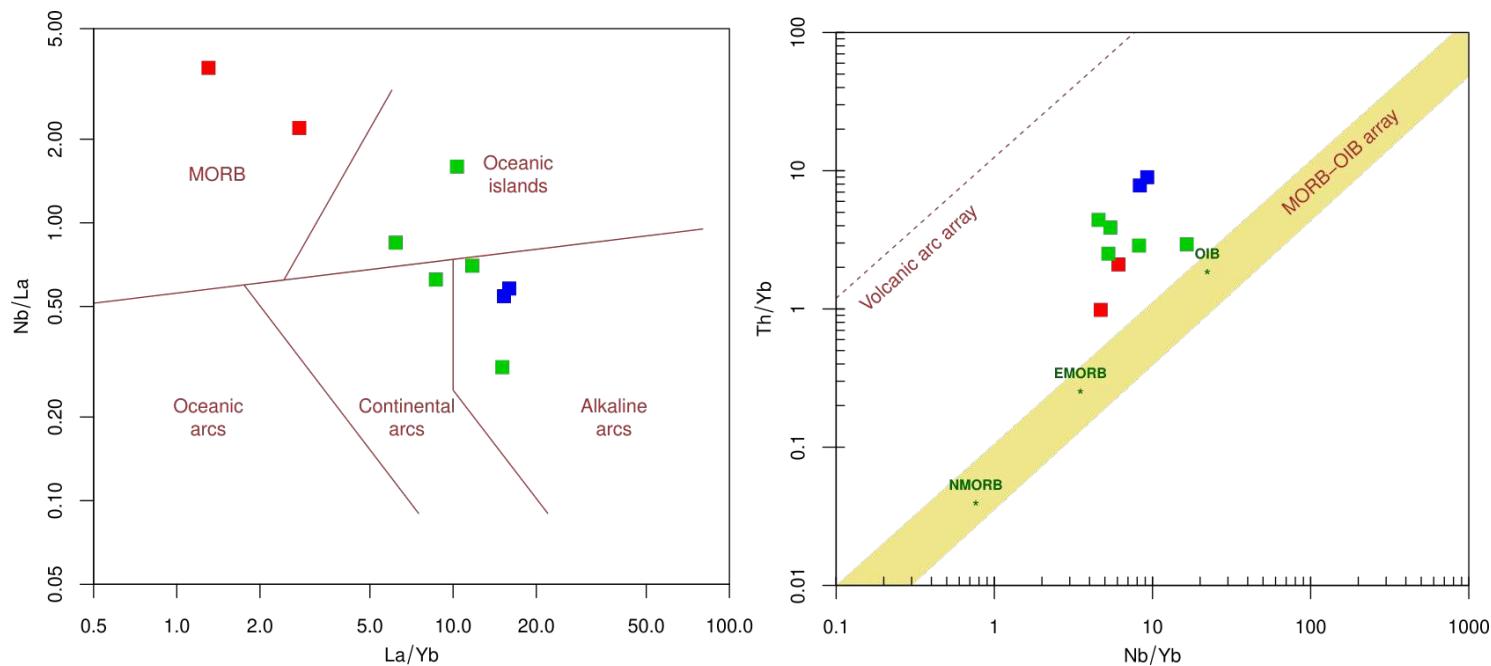
Geochemistry.

Correlation diagrams between SiO_2 and ratios of highly (Th and Nb) and moderately (La and Dy) incompatible elements over compatible element Yb. During fractional crystallization concentration of an incompatible element would increase leading to increasing ratio with the increase of SiO_2 . Dy/Yb increase indicates fractional crystallization of garnet, which implies a thick crust in the Central Pamir at the time of formation of Bartang volcanics.



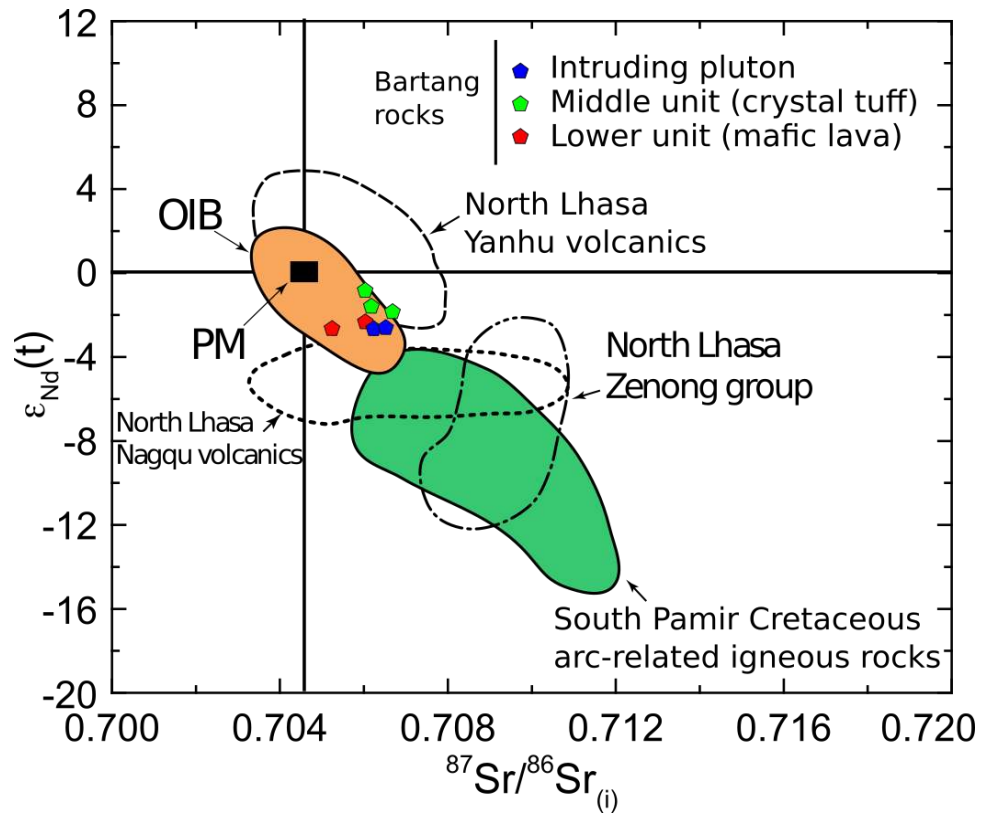
Geochemistry.

Tectonic discrimination plots for Bartang volcanic and plutonic rocks. Left (Hollocher et al., 2012). The rocks plot in the fields of MORB, Oceanic islands and Alkaline arcs. Considering the increase of La/Yb ratio with the increase of SiO₂ shown in the previous slide, this plot indicates more acidic members of the Bartang volcanic and plutonic rocks cannot reflect their tectonic setting. But lavas of lower unit plotting in the field of MORB most probably suggest an extensional tectonic setting. Right Pearce (2008). Mafic and intermediate lavas of the lower unit plot close to enriched MORB.



Radiogenic isotopes.

7 samples from the Bartang volcanics were measured for whole rock Sr-Nd radiogenic isotopic ratios. The samples yielded relatively low initial $^{87}\text{Sr}/^{86}\text{Sr}$ ratios that range between 0.705243 and 0.706702. Epsilon Nd values are negative (-0.83 – -2.66) but plot in the area of Oceanic Island Basalts' ratios. Comparison with the arc-related (Zenong group and Nagqu volcanics) and extensional (Yanhu volcanics) volcanic rocks of Lhasa terrane of Tibet and the Southern Pamir arc-related volcanic rocks indicates that the Bartang volcanics must have been formed in an extensional tectonic setting.



Conclusions.

- Dated zircon grains from the volcanic and plutonic rocks suggest a late Cretaceous to Paleogene age for the Bartang sequence.
- The geochemical properties of rocks demonstrate that a complex tectonic regime could be responsible for their formation. REE pattern of rocks similar to MORB and their enrichment in highly mobile and incompatible elements, as well as a positive Pb anomaly indicate partial melting of a metasomatized mantle source. The arc-related pattern of more felsic members of rocks have been formed as a result of fractionation of the mafic members.
- Radiogenic Sr-Nd isotopic ratios support the derivation of the Bartang magmas from a mantle source.
- Based on the review of literature, the observed geochemical and isotope-geochemical patterns of the Bartang volcanic rocks could be explained by a slab roll-back followed the collision of The Kohistan-Ladakh island arc with Eurasia in the late Cretaceous.

References

- Gale, A., Dalton, C. A., Langmuir, C. H., Su, Y., & Schilling, J. G. (2013). The mean composition of ocean ridge basalts. *Geochemistry, Geophysics, Geosystems*, 14(3), 489-518.
- Hollocher, K., Robinson, P., Walsh, E. & Roberts, D. (2012). Geochemistry of amphibolite-facies volcanics and gabbros of the Storen Nappe in extensions west and southwest of Trondheim, western gneiss region, Norway: A key to correlations and paleotectonic settings. *American Journal of Science* 312, 357–416.
- Pearce, J. A. (2008). Geochemical fingerprinting of oceanic basalts with applications to ophiolite classification and the search for Archean oceanic crust. *Lithos* 100, 14–48.
- Shand, S. J. (1943). *Eruptive Rocks. Their Genesis, Composition, Classification, and Their Relation to Ore-Deposits with a Chapter on Meteorite*. New York: John Wiley & Sons.